CHINESE OPTICS LETTERS

Vol. 21, No. 8 | August 2023

Immersed liquid cooling Nd:YAG slab laser oscillator

Zhibin Ye (叶志斌)*, Xiaolong Zhou (周小龙)**, Shu Jiang (江 舒), Meng Huang (黄 萌), Fei Wu (吴 飞), and Dongge Lei (雷冬阁)

College of Electrical and Information Engineering, Quzhou University, Quzhou 324000, China

*Corresponding author: nibihzey@zju.edu.cn

**Corresponding author: xiaolong@ieee.org

Received January 12, 2023 | Accepted April 23, 2023 | Posted Online August 2, 2023

An immersed liquid cooling slab laser is demonstrated with deionized water as the coolant and a Nd:YAG slab as the gain medium. Using waveguides, a highly uniform pump beam distribution is achieved, and the flow velocity distribution is also optimized in the channels of the gain module (GM). At various flow velocities, the convective heat transfer coefficient (CHTC) is obtained. Experimentally, a maximum output power of 434 W is obtained with an optical–optical efficiency of 27.1% and a slope efficiency of 36.6%. To the best of our knowledge, it is the highest output power of an immersed liquid cooling laser oscillator with a single Nd:YAG slab.

Keywords: liquid cooling; slab; laser oscillator; convective heat transfer coefficient.

DOI: 10.3788/COL202321.081401

1. Introduction

Generally, the solid-state laser (SSL) is developed towards achieving higher power. However, thermal effects such as thermal stress, thermal birefringence, and thermal lens continue to be major limiting factors for increasing output power while retaining good beam quality. Worst of all, as the pump power continues increasing, the tension on the gain medium may even cause a fracture. It is believed that thermal management technology has played an important role in SSL devices, and in recent years, the gain module (GM) design has received much attention in order to provide great cooling performance[1–4].

There are mainly two methods that are used to obtain effective thermal management. The first method is to create an optimum cooling system for heat extraction and transmission, which typically involves two types. One type is the liquid-conduction-cooled method, in which the gain medium is welded on the solid cooler while the surface bending caused by the slab welding process is inevitable. Furthermore, the medium with the highest heat flux cannot be cooled immediately at the pump surface, resulting in a low heat transfer efficiency. The other type is the fluid-convection-cooled method, in which the fluid circulates throughout the surfaces of the gain medium, including the pump surface, quickly and easily dissipating the heat. According to extensive research, the greatest attainable heat transfer rate for cooling using gas is roughly $5\,\mathrm{W/cm^2}$[1]. Liquid cooling, on the other hand, is more effective compared to gas cooling and is more suitable for high power SSL. It can readily manage heat fluxes of approximately $100\,\mathrm{W/cm^2}$[1]. The second method involves aligning the axis of a laser beam with the direction of the heat stream, which greatly reduces the effects of thermal lensing and constraints in the slab. Transverse temperature gradients are substantially eliminated in slab SSL with end pumping because the slab's waste heat is removed in a direction parallel to the axis of the laser beam. Furthermore, the high-aspect-ratio of the slab provides a large surface area for cooling. As a result, the slab is appropriate for high-power SSL.

Based on the analysis above, the immersed liquid cooling Nd:YAG slab laser shows great potential for thermal management in producing a high power laser because this kind of laser features the use of the liquid as coolant and slab as gain medium. The medium is immersed fully in a flowing coolant, and the heat is efficiently carried away by convection method. However, there is still few research revealing the development of an immersed liquid cooling Nd:YAG slab laser. A typical one is a 3 kW immersed liquid cooling Nd:YAG slab laser[5]. However, the channels' structure and cooling capacity inside the GM were not mentioned. The coolant's uniformity along the flow direction was not measured experimentally, either.

In this contribution, an immersed liquid cooling slab laser oscillator is devised, in which the Nd:YAG slab is cooled by deionized water flowing on the largest surfaces of it. The convective heat transfer coefficient (CHTC) is measured at various flow states experimentally. The maximum allowable thermal loads in the slab are quantitatively investigated. The performance of lasing is studied at different flowing velocities. Finally, a 434 W laser output is obtained with a pump power of 1600 W when the pump beam's uniformity is 92% and the flow velocity is around 4 m/s. The optical–optical efficiency is 27.1%.

2. Experimental Setup and Results

Figure 1 shows the experimental setup of the immersed liquid cooling Nd:YAG slab laser oscillator. It is similar to the setup in Ref. [6]. The setup uses a plano-concave cavity with a high reflector (HR), an output coupler (OC), and two dichroic mirrors (DMs). The DMs are HR coated at 1064 nm and high transmittance (HT) coated at 808 nm for light with a 45° incidence angle. The cavity mirrors (HR and OC) are positioned close to the two DMs in order to minimize the length of the cavity. Finally, the length is fixed at 20 cm. The pump beam of 808 nm wavelength emitted from the laser diode (LD) stacks is uniformed by the coupling system and projected into the GM [Figs. 1(b) and 1(c)].

2.1. Pumping system

The GM is pumped by four LD stacks, two per side, each of which consists of 30 LD bars with 54 mm × 10 mm emission areas. Figure 2(a) shows the emission beam at the exit plane by one of the stacks. Several bars have been destroyed because of long-term use, and some locations are no longer illuminated. The pump beam's central wavelength is 808 nm by controlling the temperature of the coolant. The microlens individually collimates the LD bar and the light projects on the central region of 45 mm × 18 mm in the slab by the following coupling system.

Two coupling lenses (cylindrical lenses), a rectangular waveguide, and an imaging system (IS) comprise the coupling system. The collimated pumping beams are focused into a rectangular waveguide using two coupling lenses with focal lengths of 170 mm in the fast-axis (x-axis) and 80 mm in the slow-axis (y-axis). A 100-mm-length (z-axis) planar rectangle waveguide with a width (x-axis) of 3 mm and a height (y-axis) of 7.5 mm is used to achieve excellent uniformity of pump intensity distribution. A uniform pumping region of 45 mm × 18 mm is produced in the center of the GM by developing an IS with a magnification

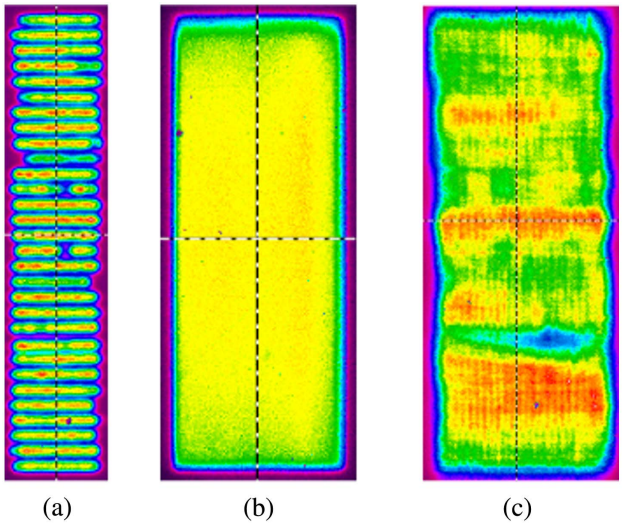

Fig. 2. Emission beam from the LD stack. (a) At the exit plane by one of the stacks, (b) using a waveguide with the uniformity of 92%, and (c) without using a waveguide with the uniformity of just 70%.

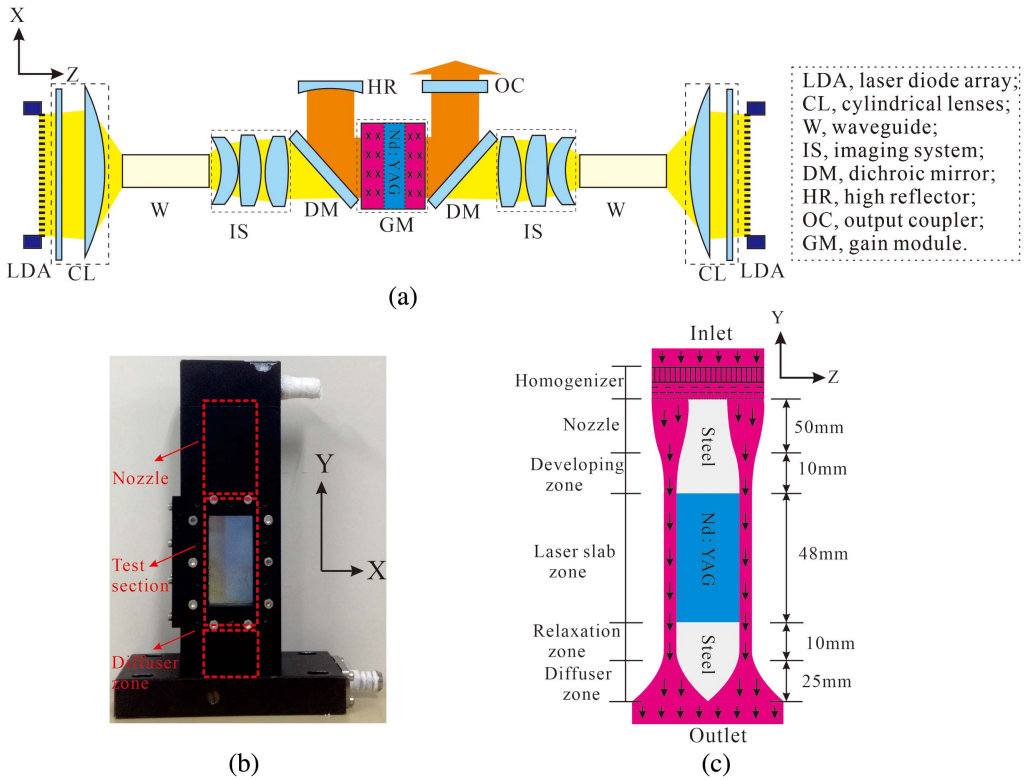

Fig. 1. (a) Immersed liquid cooling Nd:YAG slab laser oscillator, (b) the GM, and (c) the GM's internal structure.

of 6. Figure 2(b) is the final pump beam as measured by a charge-coupled device (CCD). The pump uniformity is calculated using the root mean square (RMS)[7], which is 92% in our experiment. The pump uniformity has a great influence on an oscillator's output power[5]. The temperature gradient in the slab is minimal with the increased pump uniformity, which limits thermally induced stress and beam aberration[5]. As shown in Fig. 2(c), the uniformity of the pump beam is just 70% when the rectangular waveguide is removed from the coupling system. (The IS also changes to couple the pump beam.) The efficiency of the coupling system is about 85%.

2.2. Design scheme for cooling channels

The schematics of the GM and its internal structure are depicted in Figs. 1(b) and 1(c), respectively. The GM contains two cooling channels, one Nd:YAG slab, and two windows (made of fused silica). The main reason for using deionized water as a coolant is that it is relatively cheap compared to other laser coolants. The coolant at 22°C circulates through the channels from the inlet to the outlet. The coolant runs across the slab's two large surfaces, removing the deposited heat through a convection cooling method. The slab and the windows are spaced by 0.5 mm. The dimensions of the slab are 48 mm (y) × 18 mm (x), and the real aperture of the laser beam is 45 mm × 18 mm (Both the top and bottom 1.5 mm edges of the slab are not pumped). The thickness is 2 mm. The slab is HT coated (relative to water) for 808 nm and 1064 nm while each window has one side that is (to the air side) HT coated (relative to air), and the other side (to the liquid side) is HT coated (relative to water) for 808 nm and 1064 nm.

The flow direction is along the y-axis from top to bottom, therefore the influence of the coolant gravity on the flow state can be ignored. The channel structure is identical to the experimental setup described in Ref. [6]. A flow homogenizer is used to break up bigger eddies and principally act to minimize the coolant's nonuniformities and fluctuations, as shown in Fig. 1(c). It consists of one honeycomb and three different mesh-sized screens. A three to one contraction ratio nozzle (also known as a contraction region) follows the last homogenizer screen, and its contour is determined by a fifth-order polynomial:

$$D = \left[1 - 10\left(\frac{l}{L}\right)^3 + 15\left(\frac{l}{L}\right)^4 - 6\left(\frac{l}{L}\right)^5\right] \cdot (D_1 - D_2) + D_2, \tag{1}$$

where l and D are the length and height of the nozzle, respectively; $D_1 = 1.5$ mm and $D_2 = 0.5$ mm are the heights of the nozzle at the inlet plane (where $l = 0$ mm) and the outlet plane (where $l = 50$ mm), respectively; and $L = 50$ is the total length of the nozzle, as shown in Figs. 1(b) and 1(c).

The contraction ratio is a key factor that influences the flow quality[8,9]. Following the contraction region, the flow accesses the 0.5 mm height × 18 mm width × 68 mm length test section, which is divided into three zones: the development, the laser slab, and the relaxation zones. Before the coolant crosses the laser slab zone, the development zone provides a fully developed laminar flow. The relaxation zone intends to eliminate the downstream effect and influences the coolant flowing over the slab[8–10]. As illustrated in Figs. 1(b) and 1(c), a 25-mm-long diffuser offers some pressure recovery at the test section's exit[8,11]. It has a circular curve with a half angle of 1.5°. The flow channel is primarily based on known wind tunnel designs[8–13].

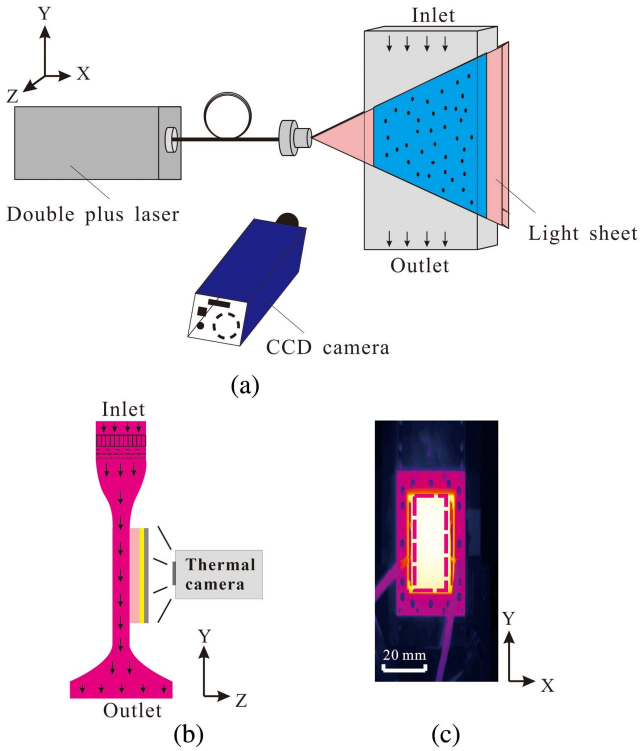

Fig. 3. (a) Setup to measure the flowing state, (b) the setup to measure the temperature distribution, and (c) the temperature distribution measured on the resistor's surface.

The structure of the channels is intended to provide laminar flow and sufficient heat transfer capacity, allowing for a high laser output power. The flowing state is measured using particle image velocimetry (PIV) technique, as shown in Fig. 3(a), and the heat transfer capacity is obtained by a single-channel experimental setup, as shown in Figs. 3(b) and 3(c). Both issues will be discussed in detail below.

2.3. Flowing state in channels

Figure 3(a) shows the PIV apparatus. It mainly consists of a double-pulse laser, a CCD camera, the seeding particles, and the fluid being investigated. The image processing device and the synchronizer are not depicted here. The fluid is seeded with trace particles, allowing the CCD camera to detect the flowing state. In the process of measurement, the double-pulse laser emits the sheet light to illuminate the entire measurement area. Two frames are quickly captured using the CCD camera. To ensure the accuracy of the cross-correlation analysis, each exposure is separated on its own frame. Both the CCD and the laser are

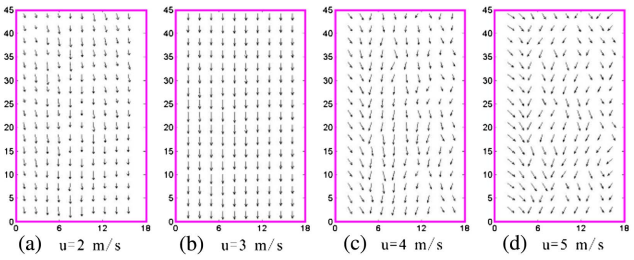

Fig. 4. Experimental results of velocity distributions for the Reynolds numbers of 1946 (u = 2 m/s), 2919 (u = 3 m/s), 3892 (u = 4 m/s), and 4865 (u = 5 m/s) in the laser slab zone.

triggered by the synchronizer, which is computer-controlled. The synchronizer can match each frame of the CCD sequence in combination with the laser firing. As a result, the duration between each laser pulse and the positioning of the laser shot in relation to the camera's timing can be precisely controlled. The time is crucial since it is used to calculate the fluid velocity distribution in the PIV analysis. References [14–16] provide a more full and complete overview of the PIV technique. The arrows represent the coolant's flowing direction, as shown in Fig. 4.

The Reynolds number (Re) is frequently employed to specify a fluid's state in fluid mechanics. Turbulent flow, transition flow, and laminar flow are represented by Re of greater than 4000, 2300–4000, and less than 2300 (theoretical threshold values). The Re is denoted by

$$\mathrm{Re} = \frac{uL}{v}, \tag{2}$$

where u is the flow velocity, L is the hydraulic channel diameter, and $v = 1 \times 10^{-6}\ \mathrm{m}^2/\mathrm{s}$ is the water's viscosity coefficient. The flow velocity can reach a maximum of 5 m/s. For a cuboidal channel,

$$L = \frac{4S}{\chi}, \tag{3}$$

where the channel's wetted perimeter is $\chi = 37$ mm and the open area is $S = 9\ \mathrm{mm}^2$. Equations (2) and (3) predict that the Re will be less than 2300 when the channel height is 0.5 mm and the flow velocity is less than 2.4 m/s. When the Re is minimal, the velocity distribution in the experiment is highly uniform [Figs. 4(a) and 4(b)]. With the increased flow velocity, the uniformity deteriorates [Figs. 4(c) and 4(d)]. Meanwhile, the fluid state first reaches the laminar state and then the turbulent state. Furthermore, instead of 2.4 m/s, the threshold flow velocity is approximately between 3 and 4 m/s. This is primarily due to the fact that the threshold Re refers to a range of numbers rather than a specific value. Overall, the flow state is uniform at low velocities (2 m/s, 3 m/s, and 4 m/s), and the flow channel design fits the requirements of laminar flow.

2.4. Channel's cooling capacity

Aside from achieving a generally uniform flow, the cooling ability is critical in determining temperature distribution and maximum permitted thermal load. It is mainly represented by CHTC. Obviously, a higher CHTC guarantees the gain medium with a higher thermal load capacity. An apparatus is built to test the CHTC at various flow velocities. The procedure is the same as that described in Ref. [6]. A platinum thin-film resistor is coated on the surfaces of a copper-block with a 1-μm-thickness and a 7.2 Ω resistance value, which is employed as a simulated heat resource. A thin insulating layer is used to isolate the resistor from the copper. The temperature distribution on the simulated heat resource is obtained using a thermal camera, as shown in Figs. 3(b) and 3(c), and the results of the temperature distributions with varying flow velocities are depicted in Fig. 5. According to the measured results, the temperature distributions are very consistent, which is mostly owing to the high thermal conductivity of copper and the uniformity of the heat resource. Figure 5 compares the average temperature with flow velocities ranging from 2 m/s to 4 m/s. With the increase of flow velocity, the temperature decreases apparently. Thus, a larger flow velocity ensures an excellent cooling capacity, which is suited for the high power immersed liquid cooling laser in consideration of achieving a high CHTC.

Because the resistor is thin enough, the temperature difference between the film resistor and the front surface would be ignored. Furthermore, we assume that all of the heat produced by the resistor is transferred by convective transfer through the copper's surface (the water side). Therefore, the Newton's law of cooling and the one-dimensional heat conduction equation can be utilized to obtain the CHTC to determine the cooling capacity:

$$h = \frac{q}{T - \frac{q.d}{\lambda_0} - T_f}, \tag{4}$$

where $q = 5.7 \times 10^4\ \mathrm{W/m}^2$ is the heat flux density, which is obtained by controlling the resistor's current; $d = 10$ mm and

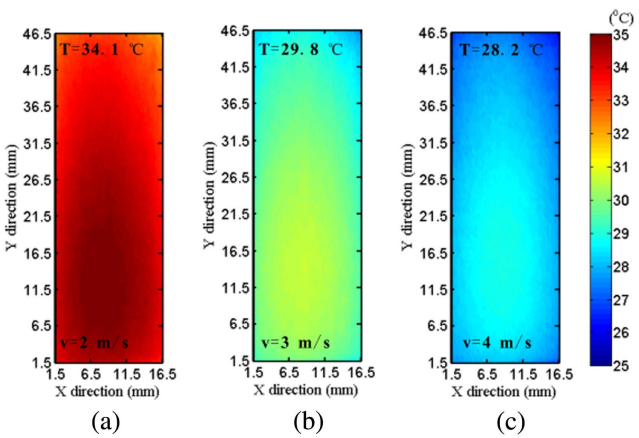

Fig. 5. Thin-film resistor's surface temperature is measured at a flow velocity of (a) 2 m/s, (b) 3 m/s, and (c) 4 m/s.

Table 1. List of the Maximum Pump Power that the Gain Medium can Sustain with Different Flow Velocities.

Flow Velocity (m/s)	Convective Heat Transfer Coefficient ($W \cdot m^{-2} \cdot K^{-1}$)	Maximum Absorbed Pump Power (W)	Maximum Temperature on the Surface of the Disk (°C)	Maximum Principal Stress (MPa)
2	5339.6	970	100	7.3
3	8941.2	1460	100	9.6
4	11,937.2	1800	100	11.0

$\lambda_0 = 387\ \mathrm{W/(m \cdot K)}$ are the copper's thickness and thermal conductivity, respectively; and T_f and T are the liquid and resistor temperatures. In the experiment, T_f was kept at 22°C.

Consider the 2 m/s flow rate as an example. Figure 6 shows the average temperature changes on the resistor's surface during the first 120 s. The temperature increases rapidly at the beginning 30 s and then gradually stabilizes to 34.1°C. The heat generated by the thin-film resistor and transformed to the liquid is balanced at this moment. Substituting $T = 34.1$°C into Eq. (4), the CHTC can be obtained at the flow velocity of 2 m/s. Table 1 shows the relationship between the CHTC and the flow velocity. The CHTC reaches 11,937.2 $W \cdot m^{-2} \cdot K^{-1}$ with a flow velocity of 4 m/s, which is roughly twice as high as the case with a velocity of 2 m/s. The following section demonstrates how the measured CHTC is used to compute the temperature distribution of the slab. Flow velocities of more than 4 m/s is not tested due to the GM's air tightness. At a flow velocity of 5 m/s, the device is prone to water leakage. When the flow rate reaches 6 m/s, the device is already leaking seriously and cannot be used, so the maximum flow rate in our experiment is designed to be 4 m/s.

2.5. Maximum permissible thermal load

It has been shown that the slab laser is a useful arrangement for achieving high output power[17,18]. Experimentally, the two big surfaces of the slab are polished, while the other four sides of the slab should not be polished so as to limit the amplified spontaneous emission (ASE). The slab's doping level is 2% (atomic fraction). The absorption efficiency reaches 94%.

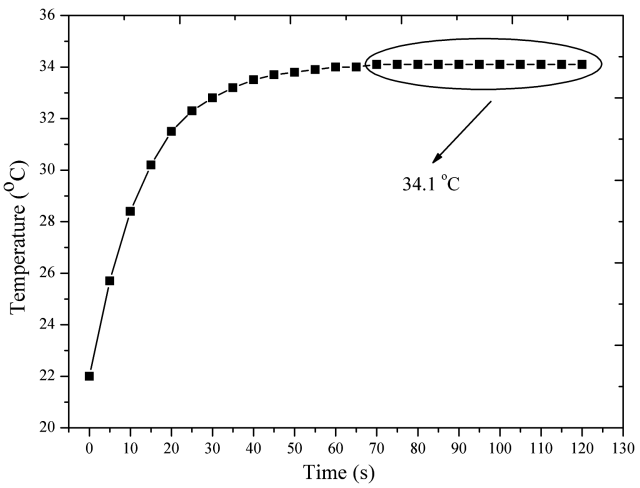

Fig. 6. Temperature changes on the resistor's surface during the first 120 s.

By taking into account that the greatest thermal stress that the Nd:YAG can withstand should be less than 130 MPa[19] and the maximum temperature on the crystal's surface must not exceed 100°C (the boiling point), we are able to determine the allowed pump power in the laser crystal. The slab's temperature and thermal stress are calculated using the finite element method. The pump power density is taken to be constant, which means that the heat power density is the same in all parts of the slab within the clear aperture. At the two large surfaces of the slab, a forced convection boundary condition is applied with the measured CHTC from the previous section and the coolant fixed temperature of 22°C. It is assumed that the slab's four side surfaces are adiabatic. Due to the flexibility of the slab and in a condition of free expansion, the external constraint surrounding it is ignored. In the analysis, the ratio of heat produced by the absorption of the pump light is fixed at 0.3, and the ratio of the total absorbed pump power is set to 94%. As indicated in Table 1, the maximum allowed absorbed pump power for a flow rate of 4 m/s is 1800 W, which is 1.86 times greater than the case of 2 m/s. It should be mentioned that the maximum pump power is governed by the highest temperature on the slab's surface rather than the maximum principal stress. Therefore, the boiling point should be considered while selecting a coolant. As a result, increasing the flow velocity may greatly improve the upper limit of the pump power. Nevertheless, a higher need for channel sealing should be offered with increased flow velocity, especially when a high-viscosity liquid is utilized.

2.6. Laser output

The experiments of the immersed liquid cooling Nd:YAG slab laser were carried out with the structures shown in Fig. 1. The flow velocity was roughly 4 m/s at the laser slab zone. Because of the stable cavity with a high Fresnel number, the laser operated in multimodes. The highest continuous-wave power of 434 W was achieved using 4-array stacks with a total pump power of 1600 W, corresponding to an optical–optical efficiency of 21.5% and a slope efficiency of 30.8%. Figure 7(a) shows the output power versus pump power curve. A higher output power can be achieved when the pump power exceeds 1600 W,

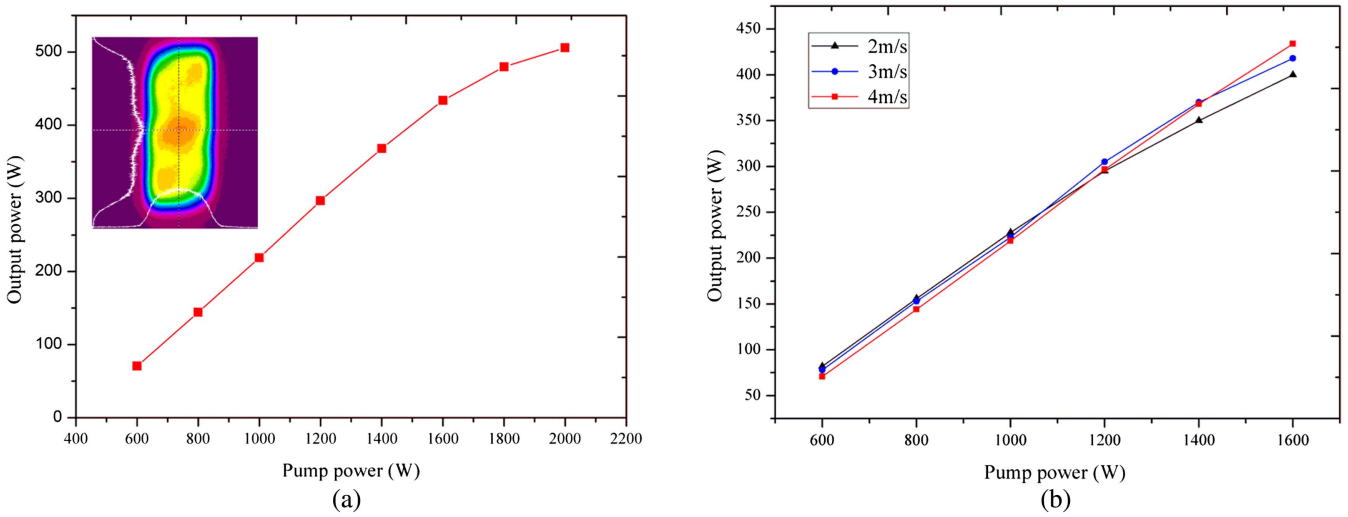

Fig. 7. (a) Output power versus the pump power and (b) the output powers at various flow velocities.

however, the output power is no longer linear. This is mostly due to the extraordinarily high coolant temperature, which is approaching the boiling point. We set the pump power at 1600 W. The near-field beam distribution of the maximum output power laser is depicted in Fig. 7(a) (top left corner). The size of the laser output was measured as 44 mm × 16 mm in the vertical and horizontal directions, respectively. The output laser can hardly be focused by a long focal lens (for instance 250 mm in the experiment), illustrating the multimode operation of the laser.

For assessing the laser performance, three different flow velocities are measured, as shown in Fig. 7(b). With the cases of 3 m/s and 4 m/s, the output powers are almost identical, and the curves have remarkable linearity and it is demonstrated that the liquid cooling removes sufficient heat. When the velocity drops to 2 m/s, the maximum output power reduces to 400 W, indicating a cooling capacity deficiency. These can be attributed to a poorer heat exchange between the coolant liquid layers and the slab. When the oscillating laser passes through the GM, it suffers from severe wavefront aberration, causing the output power to decrease continually. To avoid potential risks, operation at 1 m/s flow velocity is not tested.

3. Conclusions

We present an immersed liquid cooling Nd:YAG laser oscillator. The GM is designed to contain a Nd:YAG slab and two channels filled with the deionized water flowing across the big surfaces of the slab. A uniform flow field and pump beam distributions are obtained by the appropriate design of the flow channel and the coupling system, respectively. A method to measure the CHTC is proposed, and the maximum CHTC reaches 11,937.2 $W \cdot m^{-2} \cdot K^{-1}$ with a flow velocity of 4 m/s in the experiment. At a pump power of 1600 W, a multimode laser output of 434 W is achieved, with a slope efficiency of 36.6% and an optical–optical efficiency of 27.1%.

According to the experimental results, the immersed liquid cooling Nd:YAG slab laser oscillators have the potential to be compact and effective sources with good thermal management. With more slabs or GMs, the proposed design has the ability to increase power scaling due to the advantages of very uniform distribution of the flowing velocity and the pump beam. In order to enhance beam quality, future studies will also concentrate on the design of the unstable cavity.

Acknowledgement

This work was supported by the National Natural Science Foundation of China (No. 62105179), the Joint Funds of the Zhejiang Provincial Natural Science Foundation (No. LZY21F050001), and the Quzhou Science and Technology Plan Project (Nos. 2022K87 and 2021K40).

References

1. R. Z. Nie, J. B. She, P. F. Zhao, F. L. Li, and B. Peng, "Fully immersed liquid cooling thin-disk oscillator," Laser Phys. Lett. **11**, 115808 (2014).
2. L. Liu, N. Li, Y. Liu, C. Wang, W. Wang, and H. Huang, "1 kHz, 430 mJ, sub-nanosecond MOPA laser system," Opt. Express **29**, 22008 (2021).
3. L. Huang, Y. Zheng, Y. Guo, L. Zhang, C. Sun, and X. Wang, "21.2 kW, 1.94 times diffraction-limit quasi-continuous-wave laser based on a multi-stage, power-scalable and adaptive optics controlled Yb:YAG master-oscillator-power-amplifier system," Chin. Opt. Lett. **18**, 061402 (2020).
4. H. Yang, "Thermal effects of direct-liquid-cooled split disk laser," Opt. Laser Technol. **150**, 107945 (2022).
5. X. Fu, P. Li, Q. Liu, and M. Gong, "3 kW liquid-cooled elastically-supported Nd: YAG multi-slab CW laser resonator," Opt. Express **22**, 18421 (2014).
6. Z. Ye, C. Liu, B. Tu, K. Wang, Q. Gao, C. Tang, and Z. Cai, "Kilowatt-level direct-'refractive index matching liquid'-cooled Nd: YLF thin disk laser resonator," Opt. Express **24**, 1758 (2016).
7. P. Li, Q. Liu, X. Fu, and M. Gong, "Large-aperture end-pumped Nd: YAG thin-disk laser directly cooled by liquid," Chin. Opt. Lett. **11**, 041408 (2013).
8. P. M. Ligrani and R. D. Niver, "Flow visualization of Dean vortices in a curved channel with 40 to 1 aspect ratio," Phys. Fluids **31**, 3605 (1988).

9. P. Moonen, B. Blocken, and J. Carmeliet, "Indicators for the evaluation of wind tunnel test section flow quality and application to a numerical closed-circuit wind tunnel," J. Wind Eng. Ind. Aerodyn. **95**, 1289 (2007).
10. L. S. Han, "Hydrodynamic entrance lengths for incompressible laminar flow in rectangular ducts," J. Appl. Mech. **27**, 403 (1960).
11. R. D. Mehta, "The aerodynamic design of blower tunnels with wide-angle diffusers," Prog. Aerosp. Sci. **18**, 59 (1979).
12. R. D. Mehta and P. Bradshaw, "Design rules for small low speed wind tunnels," Aeronaut. J. **83**, 443 (1979).
13. G. Diana, S. Ponte, M. De Falco, and A. Zasso, "A new large wind tunnel for civil-environmental and aeronautical applications," J. Wind Eng. Ind. Aerodyn. **74**, 553 (1998).
14. C. D. Meinhart, S. T. Wereley, and J. G. Santiago, "PIV measurements of a microchannel flow," Exp. Fluids **27**, 414 (1999).
15. R. J. Adrian, "Twenty years of particle image velocimetry," Exp. Fluids **39**, 159 (2005).
16. R. D. Keane and R. J. Adrian, "Theory of cross-correlation analysis of PIV images," Appl. Sci. Res. **49**, 191 (1992).
17. L. Sun, T. Liu, X. Fu, Y. Guo, X. Wang, C. Shao, Y. Zheng, C. Sun, S. Lin, and L. Huang, "1.57 times diffraction-limit high-energy laser based on a Nd:YAG slab amplifier and an adaptive optics system," Chin. Opt. Lett. **17**, 051403 (2019).
18. X. Liu, C. Tan, Y. Cheng, J. Wei, M. Zhu, X. Chen, and C. Mi, "7 kHz sub-nanosecond microchip laser amplified by a grazing incidence double pass slab amplifier," Chin. Opt. Lett. **19**, 021403 (2021).
19. S. C. Tidwell, J. F. Seamans, M. S. Bowers, and A. K. Cousins, "Scaling CW diode-end-pumped Nd:YAG lasers to high average powers," IEEE J. Quantum Electron. **28**, 997 (1992).